

CrossMark  
click for updates**Cite this article:** Clarke BMN, Stiles PJ. 2015

Finite electric boundary-layer solutions of a generalized Poisson–Boltzmann equation.

*Proc. R. Soc. A* **471**: 20150024.<http://dx.doi.org/10.1098/rspa.2015.0024>

Received: 12 January 2015

Accepted: 16 April 2015

**Subject Areas:**

chemical physics, applied mathematics

**Keywords:**

sharp electric boundary layers, sharp electric double layers, critical surface charge density, Grahame equation, surface forces in electrolytes, electric stabilization of sols

**Author for correspondence:**

Peter J. Stiles

e-mail: [peter.stiles@mq.edu.au](mailto:peter.stiles@mq.edu.au)

# Finite electric boundary-layer solutions of a generalized Poisson–Boltzmann equation

Bon M. N. Clarke<sup>1</sup> and Peter J. Stiles<sup>2</sup><sup>1</sup>Department of Mathematics, and <sup>2</sup>Department of Chemistry and Biomolecular Science, Macquarie University, Sydney, New South Wales 2109, Australia

We solve the nonlinear Poisson–Boltzmann (P–B) equation of statistical thermodynamics for the external electrostatic potential of a uniformly charged flat plate immersed in an unbounded strong aqueous electrolyte. Our rather general variational formulation yields new solutions for the external potential derived from both the classical Boltzmann distribution and its heuristic Eigen–Wicke modification for concentrated symmetric electrolytes. Electrostatic potentials of these mean-field solutions satisfy a homogeneous condition at a free boundary plane parallel to the electrically conducting plate. The preferred position of this plane, characterizing the outer limit of the charged electrolyte, is determined by minimizing electrostatic free energy of the electrolyte. For a given uniform density of surface charge exceeding a well-defined and experimentally accessible threshold, we show that the generalized nonlinear P–B equation predicts a unique sharp interface separating a charged boundary layer or double layer from electroneutral bulk electrolyte. Sharp electric boundary layers are shown to be an essentially nonlinear phenomenon. In the super-threshold regime, the diffuse Gouy–Chapman solution is inapplicable and thus the Derjaguin–Landau–Verwey–Overbeek analysis, predicting electrostatic repulsion between two sufficiently separated and identically charged parallel plates must be rejected. Similar limitations restrict the applicability of the Grahame equation relating surface charge density to surface potential.

© 2015 The Authors. Published by the Royal Society under the terms of the Creative Commons Attribution License <http://creativecommons.org/licenses/by/4.0/>, which permits unrestricted use, provided the original author and source are credited.

## 1. Introduction

Electrostatic fields adjacent to electrically charged surfaces immersed in an electrolyte are important in a wide variety of applications, extending from electrochemistry, through colloid science to the biophysics of ionic atmospheres [1,2]. The classical nonlinear mean-field Poisson–Boltzmann (P–B) equation is widely accepted as a continuum model for such fields, which are described by a non-dimensional electrostatic potential function  $\psi(x)$ . This model considers the electrolyte to be composed of mobile ions regarded as point charges free to move in a spatially homogeneous dielectric continuum representing the solvent. The problem has a long history and a widely accepted diffuse solution, described for a  $z : z$  electrolyte by Gouy [3] and Chapman [4] (G–C), is given by a potential function that falls from a finite value at a planar charged surface where  $x = 0$  to zero as  $x \rightarrow \infty$ . The potential is non-zero for finite  $x$ . An important relationship between the surface charge density and surface potential of an electrical conductor was noted by Grahame [5]. There have also been many heuristic efforts to modify the P–B equation to allow for dielectric saturation [6] and finite ionic size [7–10].

At thermodynamic equilibrium, the Boltzmann distribution of mobile ions in a dielectric continuum in conjunction with the Poisson equation of classical electrostatics leads to a mean-field approximation to the charge density of electrolytic ions. The resulting P–B equation takes a general form

$$\psi'' = \frac{\kappa^2}{2} F'(\psi), \quad 0 < x. \quad (1.1)$$

Here, the positive Debye parameter  $\kappa$  describes electrolyte screening in terms of experimentally accessible quantities and is defined in appendix A. For a  $z : z$  electrolyte occupying the region  $x > 0$  adjacent to a positively charged surface at  $x = 0$ , our generalized P–B equation (1.1) describes the classical P–B equation when

$$F'(\psi) = 2 \sinh \psi, \quad 0 \leq \psi, \quad (1.2)$$

and the Eigen–Wicke (E–W) equation [7] when

$$F'(\psi) = \frac{2 \sinh \psi}{1 + \gamma(\cosh \psi - 1)}, \quad 0 \leq \psi, \quad (1.3)$$

and  $\gamma$  represents the volume fraction of identically sized ions in the electrolyte. The twice continuously differentiable function  $F(\psi)$  is assumed to satisfy the conditions

$$F(\psi) \geq 0, \quad F''(\psi) > 0, \quad F(0) = 0, \quad F'(0) = 0, \quad \lim_{\eta \rightarrow 0^+} \frac{F'(F^{-1}(\eta))}{2\sqrt{\eta}} = 1. \quad (1.4)$$

We find that  $F(\psi) = 2(\cosh \psi - 1)$ ,  $\psi \geq 0$ , for the classical P–B equation and  $F(\psi) = (2/\gamma) \log(1 + \gamma(\cosh \psi - 1))$ ,  $\psi \geq 0$ , for the E–W equation. The corresponding inverse functions are  $F^{-1}(\eta) = \operatorname{arccosh}(\eta/2 + 1)$  and  $F^{-1}(\eta) = \operatorname{arccosh}(((\exp(\gamma\eta/2) - 1)/\gamma) + 1)$ ,  $\eta \geq 0$ , for the classical P–B and E–W problems, respectively. The expression  $(F'(F^{-1}(\omega^2))/2\omega)$ ,  $\omega > 0$ , plays a pivotal role in the description of our solution to the generalized P–B equation. We define *the discriminant of F* as the function

$$D_F(\omega) = \frac{F'(F^{-1}(\omega^2))}{2\omega}, \quad \omega > 0. \quad (1.5)$$

The long-standing P–B problem is re-examined as a free boundary problem, with a constant potential  $\phi(x)$  beyond a free position  $x = X > 0$ . The electrostatic potential  $\psi(x) = \phi(x) - \phi(X)$  is defined with reference to the electrostatic potential  $\phi(X)$ . When  $X = \infty$ , and  $\psi(x) \rightarrow 0$  as  $x \rightarrow \infty$ , we refer to the solution as a *diffuse boundary-layer* solution. However, we do not assume an *a priori* value for  $X$ . The value of  $X$  must be determined to satisfy appropriate physical conditions and we determine  $X$  by minimizing a functional that is proportional to the electrostatic free energy of the region enclosing the charged electrolyte. Similar approaches have traditionally been proposed [11,12] to analyse diffuse boundary layers where the outer boundary is assumed to be fixed at infinity. We characterize a unique solution as an *extremal* for the free-energy functional.

For a uniform density of surface charge above a well-defined threshold, the functional is minimized at this extremal. We call such a solution a *sharp* or *finite boundary-layer* solution. *Sharp* solutions describe external potentials  $\psi(x)$  that fall from finite non-zero values  $\zeta$  at the surface of the charged sheet to zero at a finite distance  $X$  from this surface. Our new formalism predicts a critical surface charge density at  $x=0$ . For positive surface charge densities in *excess* of this threshold value, only *sharp* solutions of the classical P–B problem (1.2) are possible. For positive surface charge densities below this critical threshold,  $X = \infty$  and the electric boundary- or double layer is always *diffuse*. We apply standard physical interface conditions [13] for electrostatic fields at the fixed surface  $x=0$  and at the interface represented by the free boundary plane at  $x=X$ . This leads to finite boundary-layer solutions that satisfy the physical requirements of charge conservation, global electroneutrality and electrochemical equilibrium, as discussed in appendices B and D.

The extremal providing a finite boundary-layer solution to the P–B problem, appears to be new. Such non-smooth solutions are no mere mathematical artefacts. They actually provide practical solutions to variational problems. For example, an early description of a broken extremal solution to the problem of minimum surface area of revolution was given by Goldschmidt. For a planar curve joining two points that are sufficiently close together, the minimal surface of revolution is a catenoid. When the distance between these points exceeds a critical threshold, Goldschmidt's solution consists of two end discs and corresponds to the broken extremal with discontinuities at each end of the interval [14]. In higher dimensions, a similar situation is observed for the Plateau problem describing a soap bubble surface as an extremal for a multiple-integral energy-functional. Such a minimal surface may consist of adjoining smooth components corresponding to a broken extremal [14]. Where the smooth parts of the extremal intersect, there are discontinuities in first spatial derivatives.

Numerical examples illustrating the super-threshold regimes of the P–B and E–W models exhibit unusual external electric-field profiles, with sharp cut-offs, for charged surfaces immersed in aqueous electrolytes. This remarkable behaviour suggests a number of simple observations and experiments with outcomes at variance with predictions based on the traditional assumption of diffuse ionic atmospheres.

## 2. Variational formalism

We consider the electrostatic field in the region  $x > 0$  adjacent to an infinite charged planar surface located at  $x = 0$ . Although the field depends only on the single variable  $x$ , we use partial derivative notation to permit extension to non-planar geometries. Consider the functional (2.1) related to the electrostatic free energy contained in the region bounded by the planes  $x = 0$  and  $x = X > 0$ .

$$I[\psi] = - \int_0^X \left( \left( \frac{1}{\kappa} \frac{\partial \psi}{\partial x} \right)^2 + F(\psi) \right) dx = \int_0^X f(x, \psi, \psi') dx, \quad (2.1)$$

where

$$f(x, \psi, \psi') = - \left( \frac{1}{\kappa} \frac{\partial \psi}{\partial x} \right)^2 - F(\psi). \quad (2.2)$$

We seek among the piecewise smooth functions, a function  $\psi(x)$ ,  $0 < x$  for which  $I[\psi]$  is minimum. Well-known arguments from the calculus of variations [14] require that  $\psi(x)$  satisfies the Euler–Lagrange (E–L) equation in integrated form

$$\frac{\partial f}{\partial \psi'}(x, \psi(x), \psi'(x)) - \int_0^x \frac{\partial f}{\partial \psi}(s, \psi(s), \psi'(s)) ds = \text{const.} \quad (2.3)$$

Piecewise smooth solutions of this E–L equation, the so-called *broken extremals*, are admissible. On intervals where  $\psi$  is smooth, the integro-differential equation above may be differentiated to obtain the classical E–L equation (1.1) that defines the general P–B equation for the electrostatic potential. A second-order differential equation can arise as the E–L equation of more than one integral functional  $I[\psi]$ . Indeed, the problem of identifying the functionals associated with a given

second-order differential equation is the inverse problem of the calculus of variations [14]. Our choice of  $I[\psi]$  for the classical P–B equation (1.2) is now standard [11,12].

From physical considerations, we impose a Neumann boundary condition,

$$\frac{1}{\kappa} \frac{\partial \psi}{\partial x} + \alpha = 0, \quad (2.4)$$

at the charged electrically conducting surface  $x=0$ . The relationship between the non-dimensional surface charge density parameter  $\alpha$  and its physical counterpart  $\sigma$  is described in appendix A. We assume that the charged plate is positive so both  $\sigma$  and  $\alpha$  are non-negative, and  $\psi'(x) \leq 0$ . If these conventions are not satisfied, the required sign changes to our equations are easily made. How restrictive is this Neumann form of boundary condition? From the viewpoint of variational theories, Neumann boundary conditions are often selected to be the *natural* boundary conditions for a problem. However, we have an even more compelling reason for selecting such a boundary condition. Our model naturally determines a *unique* relationship between the non-dimensional or ‘reduced’ surface charge density  $\alpha$  and the non-dimensional or ‘reduced’ surface potential  $\zeta = \psi(0)$ . This relationship is not imposed *a priori*, but arises from our solution. From this point of view, the Neumann condition is equivalent to a unique inhomogeneous Dirichlet condition specifying the surface potential at  $x=0$ . Thus the Neumann condition is the more natural.

Solution of (1.1) requires a second boundary condition to be imposed. In the literature, it is assumed that  $X = \infty$  and that  $\psi(x) \rightarrow 0$  as  $x \rightarrow \infty$ . This is the *diffuse* boundary- or double-layer solution studied by many researchers. We assume only that  $X > 0$  and indeed  $X$  is free to take the value  $X = \infty$ . Hence the generalized P–B problem takes the form

$$\begin{aligned} \psi''(x) &= \frac{\kappa^2}{2} F'(\psi(x)), \quad 0 < x < X \\ \frac{1}{\kappa} \frac{\partial \psi}{\partial x}(0) + \alpha &= 0, \quad \psi(X) = 0. \end{aligned} \quad (2.5)$$

We proceed to construct a family of non-trivial solutions, determined by reduced surface potentials  $\zeta \neq 0$ .

For planar geometry, we can convert the P–B system (2.5) into a first-order differential equation. The identity

$$\psi' \left( \psi'' - \frac{\kappa^2}{2} F'(\psi) \right) = \frac{1}{2} ((\psi')^2)' - \frac{\kappa^2}{2} (F(\psi))' = 0 \quad (2.6)$$

is integrated between 0 and  $x$  to obtain

$$\left( \frac{1}{\kappa} \psi'(x) \right)^2 - \left( \frac{1}{\kappa} \psi'(0) \right)^2 = F(\psi(x)) - F(\psi(0)). \quad (2.7)$$

We introduce a *non-dimensional electric field*  $v(x) = -\kappa^{-1}(\partial\psi/\partial x)$  and use the boundary condition  $v(0) = \alpha$  to obtain the first-order differential equation

$$v(x) = \sqrt{\alpha^2 - \omega^2 + F(\psi(x))}, \quad (2.8)$$

where  $\omega = \sqrt{F(\zeta)}$  is the *transformed surface potential*. After separating variables and integrating, we find for a given  $\kappa$  that

$$x = \frac{1}{\kappa} \int_{\psi}^{F^{-1}(\omega^2)} \frac{dy}{\sqrt{\alpha^2 - \omega^2 + F(y)}}, \quad 0 \leq x \leq X, \quad (2.9)$$

which implicitly defines  $\psi(x)$ . The integral (2.9) has an upper limit equal to the reduced surface potential  $\zeta$ . It is an unusual description of the potential  $\psi(x)$  in that it defines the inverse function

$\psi^{-1}$ . Using (2.8) and (2.9), we define the non-dimensional electric field  $v(x)$  through the implicit expression

$$x = \frac{1}{\kappa} \int_{F^{-1}(v^2 - \alpha^2 + \omega^2)}^{F^{-1}(\omega^2)} \frac{dy}{\sqrt{\alpha^2 - \omega^2 + F(y)}}, \quad 0 \leq x \leq X. \quad (2.10)$$

### 3. Minimum properties of boundary-layer solutions

We have constructed in implicit form, a family of electric potentials  $\psi(x)$  and fields  $v(x)$  for the generalized P-B equation. The members of this family are determined by the non-dimensional density of surface charge  $\alpha$ . In the language of variational calculus, we have constructed a *field of extremals* for the functional  $I[\psi]$ . The appropriate choice of  $\alpha(\omega)$  is characterized by the condition that *the functional  $I[\psi]$  attains a minimum* for this family. This condition defines  $\alpha(\omega)$  uniquely, and thereby a unique potential  $\psi(x)$  satisfying (2.5).

For the G-C problem, Grahame [5] has taken the reduced density of surface charge to be  $\alpha(\zeta) = 2 \sinh(\zeta/2)$  or, for small surface potentials,  $\alpha(\zeta) = \zeta$ . We will show that the minimum condition for  $I[\psi]$  determines that  $X = \infty$  for  $\omega$  less than or equal to a threshold value. It also determines that the Grahame equation relating surface charge density to surface potential takes the form

$$\alpha(\omega) = \omega = \sqrt{F(\zeta)}. \quad (3.1)$$

We signify such diffuse solutions  $\psi_d(x)$  by using the subscript d ( $\equiv$ diffuse). For  $\omega$  greater than the threshold value, there is a unique finite  $X$  such that  $\psi(X) = 0$ . We describe such solutions  $\psi_s(x)$  as *sharp*, signified by the subscript s ( $\equiv$ sharp). The Grahame result (3.1) is inapplicable in this sharp regime. We will determine its proper replacement.

Eliminating the square of the derivative in the free-energy functional using equation (2.8),

$$I[\psi] = - \int_0^X \left( \left( \frac{1}{\kappa} \frac{\partial \psi}{\partial x} \right)^2 + F(\psi(x)) \right) dx = -(\alpha^2 - \omega^2)X - 2 \int_0^X F(\psi(x)) dx. \quad (3.2)$$

From (2.9), the boundary-layer thickness is defined by the integral

$$X = \frac{1}{\kappa} \int_0^{F^{-1}(\omega^2)} \frac{dy}{\sqrt{\alpha^2 - \omega^2 + F(y)}}, \quad 0 \leq \omega \leq \alpha \quad (3.3)$$

in which the upper limit  $F^{-1}(\omega^2) = \zeta$ . Thus, after a change of variable to  $y = \psi(x)$ , (3.2) takes the form

$$I[\psi] = - \frac{1}{\kappa} \int_0^{F^{-1}(\omega^2)} \frac{(\alpha^2 - \omega^2 + 2F(y))}{\sqrt{\alpha^2 - \omega^2 + F(y)}} dy, \quad 0 \leq \omega \leq \alpha. \quad (3.4)$$

A further change of variable  $F(y) = (\alpha^2 - \omega^2)u^2$  leads to the expression

$$I[\psi] = - \frac{(\alpha^2 - \omega^2)}{\kappa} \int_0^{\omega/\sqrt{\alpha^2 - \omega^2}} \frac{(2u^2 + 1)}{\sqrt{u^2 + 1}} \frac{1}{D_F(u\sqrt{\alpha^2 - \omega^2})} du, \quad 0 \leq \omega \leq \alpha. \quad (3.5)$$

When  $\omega = 0$

$$I[\psi] = 0, \quad (3.6)$$

and when  $\omega = \alpha$

$$I[\psi] = - \frac{2}{\kappa} \int_0^{F^{-1}(\alpha^2)} \sqrt{F(y)} dy. \quad (3.7)$$

We now determine a minimum for  $I[\psi]$  by requiring  $(\partial/\partial\omega)I[\psi] = 0$ . Differentiation of (3.4) with the aid of the Leibniz rule gives

$$\frac{\partial}{\partial\omega} I[\psi] = - \frac{(\alpha^2 + \omega^2)}{\kappa \alpha D_F(\omega)} + \frac{\omega(\alpha^2 - \omega^2)}{\kappa} \int_0^{F^{-1}(\omega^2)} (\alpha^2 - \omega^2 + F(y))^{-3/2} dy, \quad (3.8)$$

and a change of variable yields

$$\frac{\partial}{\partial \omega} I[\psi] = -\frac{(\alpha^2 + \omega^2)}{\kappa \alpha D_F(\omega)} + \frac{\omega}{\kappa} \int_0^{\omega/\sqrt{\alpha^2 - \omega^2}} \frac{(1 + u^2)^{-3/2}}{D_F(u\sqrt{\alpha^2 - \omega^2})} du. \quad (3.9)$$

### (a) Finite electric boundary-layer solutions

When  $\omega = 0$ , we see from (1.4), (1.5) and (3.8) that

$$\frac{\partial}{\partial \omega} I[\psi] = -\frac{\alpha}{\kappa}. \quad (3.10)$$

When  $\omega = \alpha$ , we find, using the standard integral  $\int_0^\infty (1 + u^2)^{-3/2} du = 1$ , that (3.9) reduces to

$$\frac{\partial}{\partial \omega} I[\psi] = -\frac{2\alpha}{\kappa D_F(\alpha)} + \frac{\alpha}{\kappa} = \frac{\alpha}{\kappa} \left(1 - \frac{2}{D_F(\alpha)}\right). \quad (3.11)$$

In (3.11),  $\alpha$  and  $\kappa$  are positive so if  $D_F(\alpha) > 2$  then  $(\partial/\partial\omega)I[\psi] > 0$  for  $\omega = \alpha$ . From the intermediate value theorem for continuous functions, it follows that  $(\partial/\partial\omega)I[\psi] = 0$  for some  $\omega_s$  in the range  $0 < \omega_s < \alpha$ . We identify  $\omega_c = \alpha_c$  satisfying

$$D_F(\alpha_c) = 2, \quad (3.12)$$

as the critical threshold for sharp solutions. For the case of the classical nonlinear P–B equation,  $\psi'' = \kappa^2 \sinh \psi$ , the explicit critical values for the reduced surface charge density and transformed surface potential follow from (3.12) as  $\alpha_c = \omega_c = 2\sqrt{3}$ .

A straightforward examination of  $(\partial/\partial\omega)I[\psi]$  shows that it is a monotone increasing function of  $\omega$  for  $\alpha > \alpha_c$  and therefore the solution  $\omega_s$  to  $(\partial/\partial\omega)I[\psi] = 0$  is unique. This argument also proves that the free-energy functional  $I[\psi]$  attains a local *minimum* at  $\omega_s$  when  $\alpha > \alpha_c$ . Figure 1 based on typical electrolyte and surface parameters, illustrates this point. For linearized P–B and E–W versions of our generalized P–B equation (1.1) describing a  $z : z$  electrolyte,  $F'(\psi) = 2\psi$ ,  $D_F(\alpha) \equiv 1$  so the threshold condition  $D_F(\alpha) = 2$  is never satisfied. Only diffuse solutions are possible for these linearized equations. Thus, *sharp finite* boundary layers are *essentially nonlinear* phenomena.

The unique finite boundary-layer solution to the free boundary problem for the generalized P–B system (2.5) is provided by the *sharp* electrostatic potential  $\psi_s(x)$  defined implicitly by

$$x = \frac{1}{\kappa} \int_{\psi_s}^{F^{-1}(\omega_s^2)} \frac{dy}{\sqrt{\alpha^2 - \omega_s^2 + F(y)}}, \quad 0 \leq x \leq X, \quad (3.13)$$

with a corresponding sharp electric field  $v_s(x)$

$$x = \frac{1}{\kappa} \int_{F^{-1}(v_s^2 - \alpha^2 + \omega_s^2)}^{F^{-1}(\omega_s^2)} \frac{dy}{\sqrt{\alpha^2 - \omega_s^2 + F(y)}}, \quad 0 \leq x \leq X. \quad (3.14)$$

The boundary-layer thickness takes the finite value

$$X = \frac{1}{\kappa} \int_0^{F^{-1}(\omega_s^2)} \frac{dy}{\sqrt{\alpha^2 - \omega_s^2 + F(y)}}, \quad 0 < \omega_s \leq \alpha. \quad (3.15)$$

In the super-threshold regime, our finite boundary-layer solution thus defines a novel relationship between the transformed surface potential  $\omega_s = \sqrt{F(\zeta_s)}$  and the reduced surface charge density

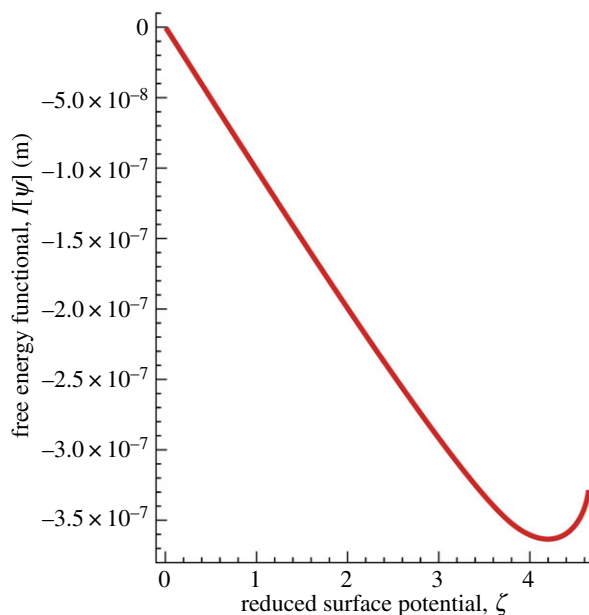


**Figure 1.** Dependence of the free-energy functional of the electrolyte on the reduced surface potential for the classical nonlinear P–B problem when the reduced surface charge density  $10 = \alpha$  is super-threshold and  $\kappa = 10^8 \text{ m}^{-1}$ . The local minimum in the hook-shaped graph defines the sharp surface potential  $\zeta_s$  in the relationship  $\omega_s = 2 \sinh(\zeta_s/2)$  and the reduced surface potential at the point of the hook satisfies  $\alpha = 2 \sinh(\zeta/2)$ . (Online version in colour.)

$\alpha(\omega_s) > \alpha_c$  superseding the Grahame result (3.1) for diffuse boundary layers. This relationship emerges from the condition  $(\partial/\partial\omega)I[\psi] = 0$  which leads, via equations (3.8) and (3.9), to

$$\Phi(\omega_s, \alpha) = -\frac{(\alpha^2 + \omega_s^2)}{\alpha\omega_s D_F(\omega_s)} + (\alpha^2 - \omega_s^2) \int_0^{F^{-1}(\omega_s^2)} (\alpha^2 - \omega_s^2 + F(y))^{-3/2} dy = 0, \quad (3.16)$$

or equivalently, after a change of variable, to

$$\Phi(\omega_s, \alpha) = -\frac{(\alpha^2 + \omega_s^2)}{\alpha\omega_s D_F(\omega_s)} + \int_0^{\omega_s/\sqrt{\alpha^2 - \omega_s^2}} \frac{(1 + u^2)^{-3/2}}{D_F\left(u\sqrt{\alpha^2 - \omega_s^2}\right)} du = 0. \quad (3.17)$$

## (b) Diffuse solutions

When the reduced surface charge density  $\alpha$  is less than or equal to the critical threshold  $\alpha_c$  of the classical P–B equation, the *diffuse* solution arises from setting  $\omega_d = \alpha \leq \alpha_c$ . In this case,  $(\partial/\partial\omega)I[\psi] < 0$  for  $0 \leq \omega \leq \alpha$  so  $I[\psi]$  reaches its minimum value at  $\omega_d = \alpha$  which determines the unique extremal  $\psi_d$  with the properties  $X = \infty$  and  $\zeta_d = F^{-1}(\alpha^2)$ . This argument establishes the Grahame equation (3.1) in the diffuse regime.

The diffuse boundary-layer potential  $\psi_d(x)$  is given implicitly by

$$x = \frac{1}{\kappa} \int_{\psi_d}^{F^{-1}(\alpha^2)} \frac{dy}{\sqrt{F(y)}}, \quad (3.18)$$

and the corresponding field  $v_d(x)$  is

$$x = \frac{1}{\kappa} \int_{F^{-1}(v_d^2)}^{F^{-1}(\alpha^2)} \frac{dy}{\sqrt{F(y)}}. \quad (3.19)$$

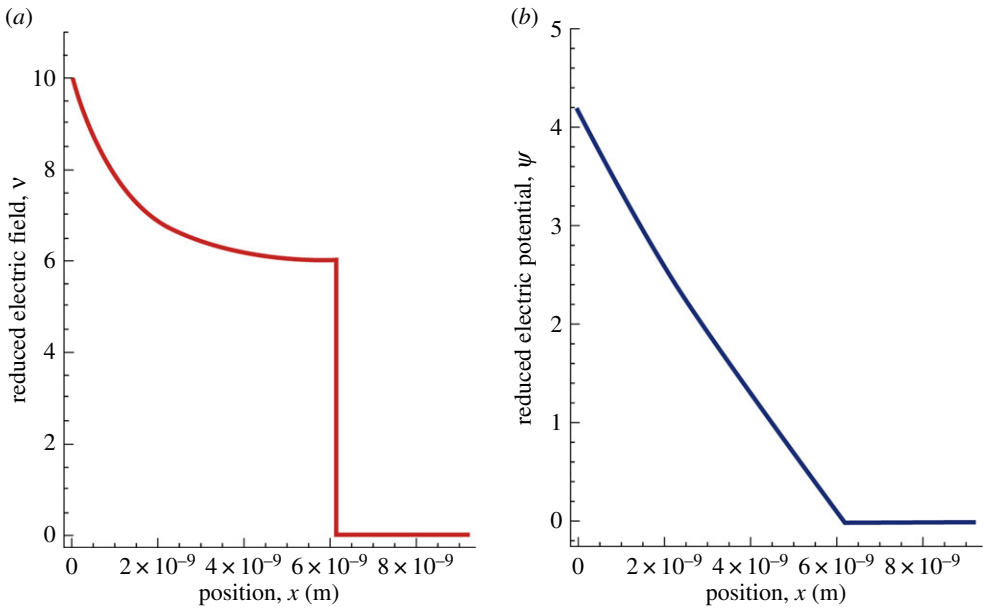


**Figure 2.** Variation of the electrostatic field (a), and the electrostatic potential (b), with distance  $x$  from the positively charged plate for the sharp super-threshold regime of the classical nonlinear P–B problem when  $10 = \alpha > \alpha_c = 2\sqrt{3}$  and  $\kappa = 10^8 \text{ m}^{-1}$ . The finite boundary layer has a thickness of 6.11 nm. (Online version in colour.)

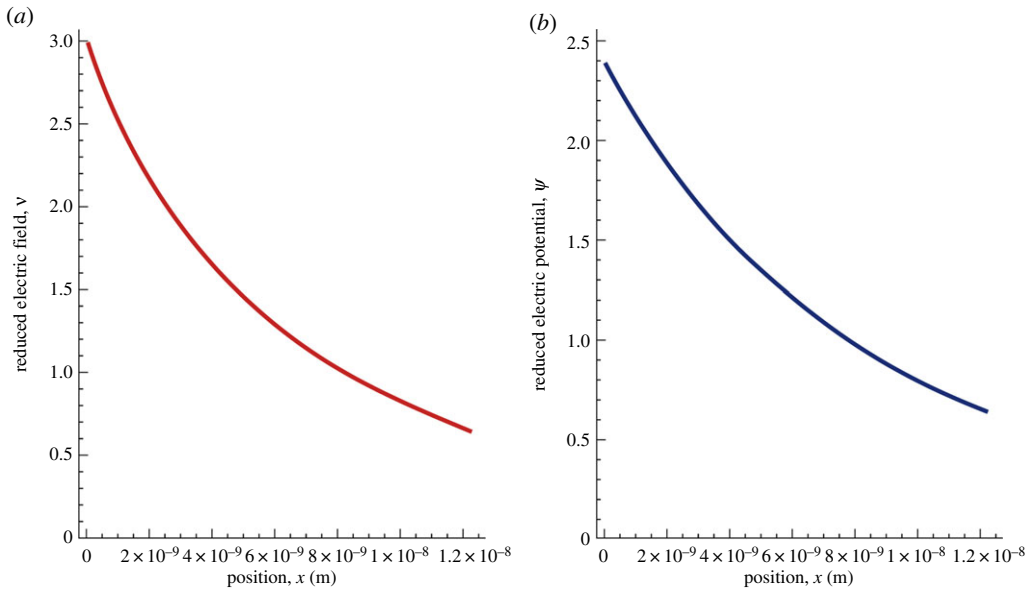


**Figure 3.** Variation of the electrostatic field (a), and the electrostatic potential (b), with distance  $x$  from the positively charged plate for the sub-threshold or diffuse regime of the classical nonlinear P–B problem when  $3 = \alpha < \alpha_c = 2\sqrt{3}$  and  $\kappa = 10^8 \text{ m}^{-1}$ . The diffuse ionic atmosphere extends to infinity. (Online version in colour.)

Typical diffuse P–B profiles corresponding to equation (3.19) for the electrostatic field and (3.18) for the electrostatic potential are shown in figure 3. The minimum value of  $I[\psi]$  in the sub-threshold regime  $\alpha \leq \alpha_c$  is given by equation (3.7) as

$$I_{\min}[\psi_d] = -\frac{2}{\kappa} \int_0^{\xi_d} \sqrt{F(y)} dy.$$

In a *diffuse* context, we see from equation (3.1) that  $F(\zeta_d) = \alpha^2$ . Thus, the reduced differential capacitance is given by

$$\frac{d\alpha}{d\zeta_d} = \frac{F'(\zeta_d)}{2\alpha} = \frac{F'(\zeta_d)}{2\sqrt{F(\zeta_d)}} = D_F(\alpha). \quad (3.20)$$

For the classical P–B equation  $F(\psi) = 2(\cosh \psi - 1)$  so the reduced differential capacitance is given by the standard Grahame expression,  $\cosh(\zeta_d/2)$ . The *diffuse* result given by equation (3.20) can be extended, by implicit differentiation, into the sharp regime. This is discussed in appendix C.

## 4. Discussion

We have characterized the generalized P–B system (2.5) as a free boundary variational problem and have constructed a unique analytical solution which provides a minimum for a free-energy functional  $I[\psi]$ . We have also shown that for *super-threshold* reduced surface charge densities  $\alpha > \alpha_c$  the solution  $\psi = \psi_s$  takes the form of a *sharp* finite boundary layer of thickness  $X$ . For *sub-threshold* charge densities  $\alpha \leq \alpha_c$ , the *diffuse* solution (figure 3) to the P–B equation for a symmetric  $z : z$  electrolyte is identical to the G–C solution [3,4]. We have found that *finite* or *sharp* boundary layers are *nonlinear* phenomena. Thus, when the classical P–B equation is linearized, as in the analysis of Debye & Hückel [15] for the electrostatic potential outside small spherical ions, only *diffuse* solutions survive.

Our use of the symbol  $\zeta$  for the reduced surface potential conforms to the notation of Verwey & Overbeek [16]. The same symbol is used for the electrokinetic potential of a colloidal particle at the ‘surface of shear’ in electrophoretic experiments [17]. Although experimental numerical estimates of these two quantities appear to be similar, our surface potential is strictly an equilibrium property.

We now consider how our new formalism modifies traditional solutions to the classical P–B problem first considered by Gouy [3] and Chapman [4]. The critical threshold, above which a diffuse boundary layer for the P–B equation (1.2) contracts to a sharp boundary layer, has been derived as  $\alpha_c = \omega_c \equiv 2 \sinh(\zeta_c/2) = 2\sqrt{3}$ . The corresponding critical reduced surface potential  $\zeta_c$  is 2.6339 regardless of the value of the Debye screening parameter. From equation (A 2), we see that this translates at 25°C to a critical surface potential of 67.67 mV for a 1 : 1 electrolyte, a value typical of surface potentials encountered experimentally. Thus, the conventional assumption of diffuse boundary layers is invalid for numerous practical problems describing thermodynamic equilibrium in electrochemistry [1] and interface science [2].

As we enter the super-threshold regime of the classical P–B equation (1.2), the magnitude of the reduced surface potential  $\zeta$  exceeds 2.6339, the boundary layer becomes sharp and its thickness  $X$  contracts rapidly. A plot of the boundary-layer thickness as a function of the transformed surface potential, deduced from our equation (3.3) for  $\kappa = 10^8$  is shown in figure 4.

Let us now consider a flat plate with a uniform density of surface charge  $\sigma = 17.8 \text{ mC m}^{-2}$ , corresponding, at 25°C to  $\alpha = 10$ , immersed in a strong 1 : 1 aqueous electrolyte with  $\kappa = 10^8 \text{ m}^{-1}$  (or a Debye screening length of 10 nm). For this example, figure 1 displays a *local* minimum when  $I[\psi]$  is plotted from (3.4) as a function of the surface potential  $\zeta$ . We see that the sharp super-threshold value of the dimensionless surface potential  $\zeta_s = 4.185$  so the corresponding dimensional surface potential is 107.5 mV at 25°C. From equation (3.15) or figure 4, the boundary-layer thickness  $X$  at equilibrium is 6.11 nm. In the well-studied sub-threshold regime, the dependence of the electric free energy on  $\zeta_d$  has been analysed by Verwey & Overbeek [16]. In contrast to the results of our super-threshold analysis (figure 1), the free-energy functional  $I[\psi_d] = -8(\cosh(\zeta_d/2) - 1)/\kappa$  in the sub-threshold regime always falls monotonically as the magnitude of  $\zeta_d$  increases. It is illuminating to examine the structure of the super-critical electric field outside this uniformly charged plate after a state of thermodynamic equilibrium has been attained. Figure 2a displays the reduced external electric field  $v(x) = -\kappa^{-1}(\partial\psi/\partial x)$ , defined by equation (3.14). The electric-field profile decreases monotonically from its boundary value  $v(0)$  to  $v(X)$  at the outer edge of the double layer where  $v'(X) = 0$ . Beyond this plane, the electric field

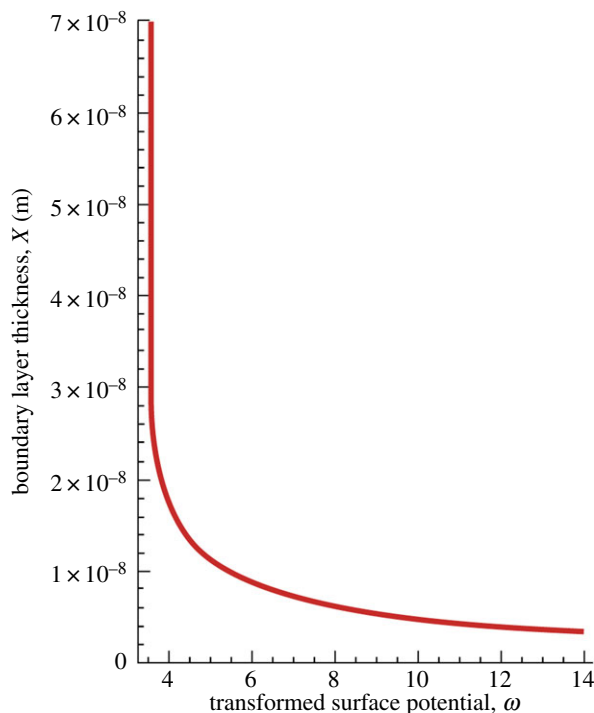


**Figure 4.** Dependence of the finite boundary-layer thickness on the transformed surface potential  $\omega = 2 \sinh(\zeta/2) > 2\sqrt{3}$  in the super-threshold regime for the classical nonlinear P–B problem when  $\kappa = 10^8 \text{ m}^{-1}$ . As  $\omega$  decreases towards its lower limit of  $\omega_c = 2\sqrt{3}$ , the thickness of the sharp layer climbs very rapidly and the electric boundary layer eventually becomes diffuse. (Online version in colour.)

falls precipitously to  $v(x) = 0$  for all  $x > X$ . In contrast to the diffuse external field displayed in figure 3*a*, the corresponding electric-field profile for a finite boundary layer displayed in figure 2*a*, is discontinuous at  $x = X$ . Both  $\psi_s(x)$  and  $\psi_d(x)$  depicted in figures 2*b* and 3*b* are continuous for all  $x > 0$ , but  $\psi_s(x)$  has a discontinuous slope at  $x = X$ .

The unusual profile exhibited in figure 2*a* has remarkable experimental implications. Consider two identical and parallel charged plates separated by a rectangular prism of electrolyte of thickness  $d$ . If  $d > 2X$ , the electric field of the first plate vanishes at every local charge associated with the second plate. Therefore, in this super-threshold regime, whenever  $d > 2X$  there is no electrostatic repulsion between the two plates of like charge! The Derjaguin–Landau–Verwey–Overbeek argument [16,17], predicting electrostatic repulsion between two identically charged plates regardless of their separation  $d$  was based on considerations restricted to diffuse double layers. It is therefore inapplicable to the situation where the plate-separation  $d$  exceeds twice the sharp boundary-layer thickness. In the absence of electrostatic repulsion, attractive London–Casimir–Polder dispersion forces associated with electron–electron correlations [18,19] can be expected to lead to weak net inter-plate attraction that is augmented by ion–ion correlations [20]. It would therefore be helpful to measure the force between two such plates as a function of  $d$  in experiments where our critical threshold for sharp boundary layers is exceeded. If  $d$  is initially large, and is gradually reduced, we anticipate that weak attraction between the plates suddenly gives way to significant repulsion for  $d < 2X$ . Such an experiment would be useful for estimating the magnitude of the boundary-layer thickness  $X$ .

Our preliminary calculations suggest that sharp boundary layers in the vicinity of electrically conducting spherical surfaces also form beyond thresholds in the critical surface charge density or surface potential. Hydrophobic colloidal suspensions such as gold nanoparticles dispersed in

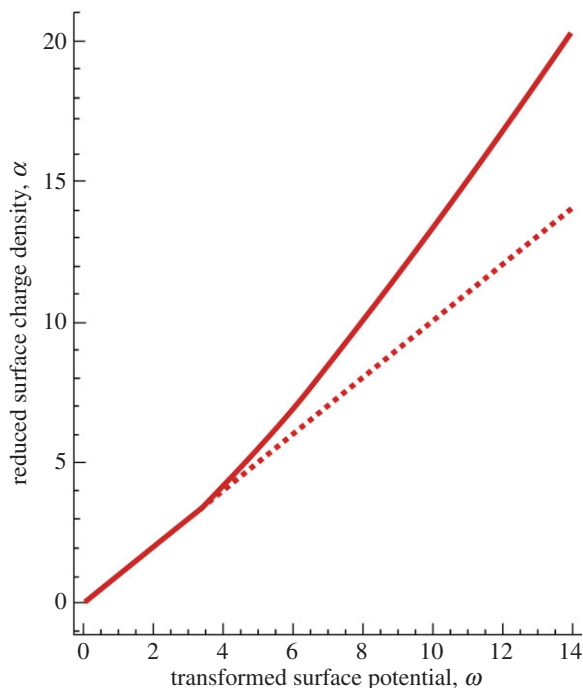


**Figure 5.** Dependence of the reduced density of surface charge  $\alpha$ , on the surface potential  $\omega$  for the classical nonlinear P–B problem. For  $\omega < \omega_c = 2\sqrt{3}$ , we have the sub-threshold Grahame equation  $\alpha = \omega = 2 \sinh(\zeta/2)$  for diffuse electric boundary layers. This graph shows that in the super-threshold regime where  $\omega > \omega_c$ , the Grahame expression, indicated by the dashed line, increasingly underestimates surface charge density as the surface potential rises. (Online version in colour.)

strong aqueous electrolytes are thermodynamically unstable with respect to particle coalescence, aggregation and sedimentation but are currently believed to be kinetically stabilized by the potential energy barrier provided by overlap of the diffuse double layers on adjacent particles. This electrostatic stabilization is pronounced when the repulsive barrier between two particles is large compared with typical thermal energies of order  $k_B T$ , where  $k_B$  is the Boltzmann constant. As noted by Derjaguin & Landau [17], this barrier, representing the sum of the positive electrostatic repulsive energy and the negative van der Waals attractive energy, is often sufficient to confer significant temporal stability to a hydrophobic colloidal suspension composed of identical particles. If as the ionic strength of the ambient electrolyte is raised, the surface charge density of the spherical colloidal particles exceeds the critical threshold, the resulting cut-off in the external radial electrostatic field (analogous to that depicted in figure 2) completely eliminates the repulsive barrier for particle separations  $r > 2R_s$ , where  $R_s$  is the outer radius of the sharp boundary layer. The stabilizing inter-particle potential energy barrier is then reduced and aggregation of the hydrophobic suspension is more rapid.

We next compare a plot of  $\alpha(\omega_s)$  with the sub-threshold Grahame result  $\alpha = \omega_d$  for which  $0 < \omega_d < \omega_c$ . For our generalized P–B equation, the super-threshold relationships (3.16) and (3.17) do not express  $\alpha$  as an explicit function of  $\omega_s$  in terms of elementary functions. Nevertheless, these implicit relationships, taking the form  $\Phi(\omega_s, \alpha) = 0$ , provide a perfectly adequate tool for numerical purposes. In the case of the classical P–B model, the slope of the contour  $\Phi(\omega_s, \alpha) = 0$  in the upper curve of figure 5 defines relevant differential capacitances with respect to the transformed surface potential. We observe that the upper finite boundary-layer curve deviates smoothly from the traditional Grahame curve in the super-threshold region  $\omega > \alpha_c$ .

Finally, we consider a brief analysis of the novel super-threshold regime for the E–W equation (1.3). Our calculations suggest that for strong 1:1 aqueous electrolytes, this regime is

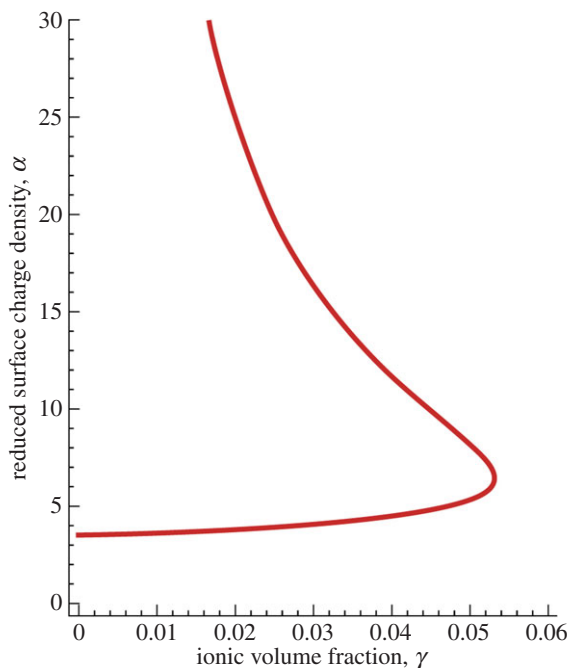


**Figure 6.** Dependence of the critical density of surface charge  $\alpha_c$ , on the volume fraction  $\gamma$  of ions in the symmetric electrolyte deduced from the E–W model. The maximum possible value of  $\gamma$  on this contour is 0.0534. When  $\gamma$  is fixed at a value moderately below this threshold, there are two critical values  $\alpha_{1c}, \alpha_{2c}$  and a finite electric boundary-layer regime is defined by  $\alpha_{1c} < \alpha < \alpha_{2c}$ . When  $\gamma = 0$ , we recover the classical P–B model. (Online version in colour.)

restricted to values of the volume-fraction  $\gamma < 0.0534$ . For more concentrated aqueous electrolytes and molten salts, our analysis of the E–W equation (1.3) indicates that the electric boundary layer is diffuse. In this diffuse regime, we have confirmed the results of Kornyshev [9] and have found that similar behaviour occurs in the sharp regime where  $\gamma < 0.0534$ . When  $\gamma < 0.0534$ , there are sharp boundary-layer regions of  $\gamma - \alpha$  parameter space in which the reduced differential capacitance is given by equation (C 3) of appendix C rather than the simpler diffuse result (3.20). Figure 6 plots the critical surface charge density satisfying (3.12) as a function of  $\gamma$ . The region to the left of the contour in  $\gamma - \alpha$  parameter space defines the finite boundary-layer regime for the E–W model. The remainder of this  $\gamma - \alpha$  parameter space defines the conventional diffuse regime explored previously [8,9]. If the concentration of a strong aqueous solution of KCl is  $1000 \text{ mol m}^{-3}$  at  $25^\circ\text{C}$ , the reciprocal Debye screening length is  $3.3 \times 10^9 \text{ m}^{-1}$ , and extant data [21] suggest that for this value of  $\kappa$  the volume fraction  $\gamma$  of this binary electrolyte is about  $2.7 \times 10^{-2}$ . Figure 6 shows that when  $\gamma = 2.7 \times 10^{-2}$ , there are two distinct values,  $\alpha_{1c} = 4.03$  and  $\alpha_{2c} = 18.3$ , of  $\alpha_c$  that satisfy the critical condition (3.12). If  $\omega \leq \omega_{1c}$  or if  $\omega \geq \omega_{2c}$ , we expect diffuse double-layer behaviour. As the surface potential  $\omega$  increases within the sharp regime  $\omega_{1c} < \omega < \omega_{2c}$ , the differential capacitance of a sharp boundary layer initially rises slightly above the estimate from equation (3.20) for diffuse boundary layers, then falls below it and finally returns to it when  $\omega = \omega_{2c}$ .

## 5. Concluding remarks

We anticipate that these hitherto overlooked finite electric boundary-layer solutions of both the classical P–B equation and its heuristic E–W modification will find numerous applications in the science of electrolyte solutions at charged interfaces.

**Data accessibility.** Calculations based on standard physical constants were performed using Wolfram's MATHEMATICA v. 10.

**Funding statement.** Each author was self-funded.

**Author contributions.** B.M.N.C.: Mathematical structure incorporating both the canonical P–B model and its E–W modification; elucidation of mathematical structure of variational solutions; introduction of a precise discriminant condition to detect earlier numerically suggested thresholds; original draft of paper. P.J.S.: Conception of the original investigation involving numerical simulations suggesting new phenomena; exploration of historical and recent literature; physico-chemical consequences of the new solutions; final drafts of paper. All other components were subject to joint investigation; numerical calculations were usually carried out by one or other of us and independently checked by the other author. Both authors gave final approval for publication.

**Conflict of interests.** We have no competing interests.

## Appendix A. Definitions and conversions to variables in SI units

Reciprocal Debye screening length of a  $z : z$  electrolyte:

$$\frac{\kappa}{\text{m}^{-1}} = \sqrt{\frac{2z^2 F^2 \bar{c}}{\varepsilon_0 \varepsilon_r RT}}. \quad (\text{A } 1)$$

Electrostatic potential:

$$\frac{\Psi(x)}{\text{V}} = \frac{RT}{|z|F} \psi(x). \quad (\text{A } 2)$$

Density of surface charge:

$$\frac{\sigma}{\text{C m}^{-2}} = \alpha \sqrt{2 \varepsilon_0 \varepsilon_r \bar{c} RT}. \quad (\text{A } 3)$$

Electrostatic free energy<sup>1</sup> of electrolyte per unit area of charged plate:

$$\frac{G}{\text{J m}^{-2}} = \bar{c} RT I[\psi], \quad (\text{A } 4)$$

where  $z$  denotes ionic valence;  $F$ , Faraday constant;  $\bar{c}$ , concentration of electrolyte in  $\text{mol m}^{-3}$  or  $\text{mM}$  units;  $\varepsilon_0$ , electric permittivity of free space;  $\varepsilon_r$ , relative permittivity of solvent (78.5 for water at 25°C);  $R$ , gas constant;  $T$ , absolute temperature.

## Appendix B. Charge conservation and electroneutrality

These principles are well established for diffuse boundary layers or double layers. We consider here only the super-threshold case that can arise when the generalized P–B equation is nonlinear.

Initially, the conducting plate at  $x=0$  and the electrolyte in which the plate is immersed are assumed to be electrically neutral. An electrochemical equilibrium, in which cations are preferentially adsorbed onto the surface of the plate, is assumed to develop. We expect charge conservation to ensure that the total charge of the system (surface charge on the plate + space charge in electrolyte + surface charge on the interface at  $x=X$ ) remains zero at equilibrium.

We use a standard pill-box argument and consider a cylinder of height  $X$  and with cross-sectional area  $A$  on the planes  $x=0$  and  $x=X$ , lying in the boundary layer and oriented so that its axis is parallel to  $x$ . The equilibrium values of the surface charge density and reduced surface charge density at  $x=0$  are  $\sigma$  and  $\alpha$ , respectively; the reduced surface potential is  $\zeta$  and the transformed surface potential is  $\omega = \sqrt{F(\zeta)}$ . By symmetry, the electric field is oriented in the direction of the  $x$ -axis and has no component orthogonal to the curved surface of the cylinder. The electric displacement  $\mathbf{D}$  at an interface bearing a density  $\sigma_i$  of surface charge satisfies the standard

<sup>1</sup>Relative to the electrolyte when  $\psi(x)=0$ .

jump condition [13]

$$(\mathbf{D}_2 - \mathbf{D}_1) \cdot \hat{\mathbf{n}} = \sigma_i. \quad (\text{B } 1)$$

Here,  $\mathbf{D}_2$  (or  $\mathbf{D}_1$ ) is the displacement vector immediately to the right (or left) of the interface with an outwardly directed normal unit vector  $\hat{\mathbf{n}}$  pointing from region 1 to region 2. As the electric field is zero and  $\psi(x) = 0$  in the region  $x > X$ , this bulk region of the electrolyte remains electrically neutral. Using the jump condition at the interfaces  $x = 0$  and  $x = X$ , we see that the positive surface charge density at  $x = 0$  is determined from the boundary condition (2.4) and is proportional to

$$-\psi'(0) = \kappa\alpha. \quad (\text{B } 2)$$

Similarly, equation (2.8) in conjunction with the interface condition  $\psi(X) = 0$  shows that the negative surface charge density at  $x = X$  with the same proportionality factor is

$$\psi'(X) = -\kappa\sqrt{\alpha^2 - \omega^2}. \quad (\text{B } 3)$$

The total charge on the flat surfaces of the cylinder is therefore proportional to

$$A(\psi'(X) - \psi'(0)) = \kappa A \left( \alpha - \sqrt{\alpha^2 - \omega^2} \right). \quad (\text{B } 4)$$

Maintaining the constant of proportionality, we directly evaluate the space charge in the electrolyte by integrating the charge density,  $-(\kappa^2/2)F(\psi)$  over the volume of the cylinder. From the first integral of equation (1.1) as given by equation (2.8),

$$\begin{aligned} -A \int_0^X \frac{\kappa^2}{2} F(\psi(x)) \, dx &= \frac{\kappa A}{2} \int_0^X \frac{1}{v(x)} \frac{d}{dx} (F(\psi(x))) \, dx \\ &= \frac{\kappa A}{2} \int_0^X (\alpha^2 - \omega^2 + F(\psi(x)))^{-1/2} \frac{d}{dx} (F(\psi(x))) \, dx. \end{aligned} \quad (\text{B } 5)$$

After a change of integration variable to  $u = F(\psi(x)) = (v(x))^2 - \alpha^2 + \omega^2$ , equation (B 5) reduces to

$$\begin{aligned} -A \int_0^X \frac{\kappa^2}{2} F(\psi(x)) \, dx &= \frac{\kappa A}{2} \int_{F(\xi)}^0 (\alpha^2 - \omega^2 + u)^{-1/2} \, du \\ &= -\frac{\kappa A}{2} \int_0^{\omega^2} (\alpha^2 - \omega^2 + u)^{-1/2} \, du = -\kappa A \left( \alpha - \sqrt{\alpha^2 - \omega^2} \right). \end{aligned} \quad (\text{B } 6)$$

Thus, in the boundary-layer region  $0 \leq x \leq X$ , the sum of surface and space-charges

$$A(\psi'(X) - \psi'(0)) - (A\kappa^2/2) \int_0^X F(\psi(x)) \, dx = 0. \quad (\text{B } 7)$$

and the system of interest remains globally electroneutral, as expected.

## Appendix C. Super-threshold generalization of the Grahame equation

For our generalized P–B system, we show that the condition  $(\partial/\partial\omega)I[\psi] = 0$  defines a unique function  $\alpha(\omega)$ ,  $\omega > \omega_c$ , relating the reduced surface charge density  $\alpha$  to the transformed surface potential  $\omega$ . This is achieved by verifying that for any solution  $(\omega^*, \alpha^*)$  to  $(\partial/\partial\omega)I[\psi] = 0$ ,  $\omega^* > \omega_c$ , the conditions of the implicit function theorem are satisfied, and hence in a neighbourhood  $N(\omega^*)$  there exists a unique continuously differentiable function  $\alpha$ , such that  $\alpha(\omega^*) = \alpha^*$  and the solution  $(\omega, \alpha(\omega))$  satisfies  $(\partial/\partial\omega)I[\psi] = 0$  for all  $\omega \in N(\omega^*)$ .

We have shown that the condition  $(\partial/\partial\omega)I[\psi] = 0$  can be written as

$$0 = \Phi(\omega, \alpha) = -\frac{(\alpha^2 + \omega^2)}{\alpha \omega D_F(\omega)} + (\alpha^2 - \omega^2) \int_0^{F^{-1}(\omega^2)} (\alpha^2 - \omega^2 + F(y))^{-3/2} \, dy \quad (\text{C } 1)$$

for  $\omega > \alpha_c$ , and  $\alpha > \alpha_c$ . Under these conditions,  $\Phi(\omega, \alpha)$  is continuous, with continuous first partial derivatives  $\Phi_\omega(\omega, \alpha)$ ,  $\Phi_\alpha(\omega, \alpha)$  and  $\Phi_{\alpha\alpha}(\omega, \alpha) \neq 0$ . From the implicit function theorem, for

any solution  $(\omega^*, \alpha^*)$  with  $\Phi(\omega^*, \alpha^*) = 0$ ,  $\omega^* > \alpha_c$ ,  $\alpha^* > \alpha_c$ , there is a neighbourhood  $N(\omega^*)$  and a continuously differentiable function  $P$  defined on  $N(\omega^*)$ , such that

$$P(\omega^*) = \alpha^*, \quad P'(\omega^*) = -\frac{\Phi_\omega(\omega^*, \alpha^*)}{\Phi_\alpha(\omega^*, \alpha^*)}, \quad \Phi(\omega, P(\omega)) = 0, \quad \text{for all } \omega \in N(\omega^*). \quad (\text{C } 2)$$

The relationship  $\Phi(\omega, \alpha) = 0$  defines a super-threshold generalization of the Grahame equation [5] as  $\alpha = P(\omega)$ ,  $\omega \in N(\omega^*)$ .

The differential capacitance is given by

$$\frac{d\alpha}{d\zeta} = \frac{d\alpha}{d\omega} \frac{d\omega}{d\zeta} = -\frac{\Phi_\omega(\omega, \alpha)}{\Phi_\alpha(\omega, \alpha)} \frac{d}{d\zeta} \left( \sqrt{F(\zeta)} \right) = -\frac{\Phi_\omega(\omega, \alpha)}{\Phi_\alpha(\omega, \alpha)} D_F(\omega), \quad (\text{C } 3)$$

at each  $(\omega, \alpha)$  on the super-threshold contour  $\Phi(\omega, \alpha) = 0$ . Note that equation (C 3) is the super-threshold generalization of the sub-threshold result (3.20).

## Appendix D. Equilibrium between ions in the boundary layer and in the bulk electrolyte

When, for the classical P–B problem, the critical threshold is exceeded, ions within the charged double layer remain in electrochemical equilibrium with those in the bulk electroneutral electrolyte where  $x > X$ . If this condition is satisfied, the electrochemical potential of the cationic or anionic species takes the same value inside the boundary layer and the bulk solution. From the Boltzmann distribution, the concentration of an ionic species at the position  $x$  outside a positively charged plate is given by  $c(x) = \bar{c} \exp[\mp z\psi(x)]$  for cations (negative sign) and anions (positive sign). Here,  $\bar{c}$  is the constant bulk concentration of the electrolyte for  $x \geq X$ . As the electrostatic potential  $\psi(x)$  is continuous at the interface  $x = X$ , ionic concentrations are also continuous across this plane. After converting the reduced electrostatic potential  $\psi(x)$  to the dimensional electrostatic potential  $\Psi(x)$  (see appendix A), we find that the natural logarithm of the Boltzmann distribution gives

$$RT \log[c(x)] + zF\Psi(x) = RT \log \bar{c}. \quad (\text{D } 1)$$

The concentration of the electrolyte throughout the bulk region  $x \geq X$  takes the fixed value  $\bar{c}$ . In an ideal electrolyte, the reference electrochemical potential  $\mu^*$  of an ionic species is a function of temperature alone, so electrochemical potentials for cations or anions at fixed temperature  $T$  take the form

$$\mu(x) = \mu^* + RT \log[c(x)] + zF\Psi(x) = \mu^* + RT \log \bar{c} = \text{const.} \quad (\text{D } 2)$$

for all  $x > 0$ .

## References

1. Bard AJ, Faulkner LR. 2000 *Electrochemical methods: fundamentals and applications*, 2nd edn. New York, NY: Wiley.
2. Butt H-J, Graf K, Kappl M. 2013 *Physics and chemistry of interfaces*, 3rd edn. Weinheim, Germany: Wiley-VCH.
3. Gouy M. 1910 Sur la constitution de la charge électrique à la surface d'un électrolyte. *J. Phys.* **9**, 457–468. (doi:10.1051/jphystap:019100090045700)
4. Chapman DL. 1913 A contribution to the theory of electrocapillarity. *Phil. Mag.* **25**, 475–481. (doi:10.1080/14786440408634187)
5. Grahame DC. 1947 The electric double layer and the theory of electrocapillarity. *Chem. Rev.* **41**, 441–501. (doi:10.1021/cr60130a002)
6. Booth F. 1951 The dielectric constant of water and the saturation effect. *J. Chem. Phys.* **19**, 391–394. (doi:10.1063/1.1748233)
7. Eigen M, Wicke E. 1954 The thermodynamics of electrolytes at higher concentration. *J. Phys. Chem.* **58**, 702–714. (doi:10.1021/j150519a007)

8. Kralj-Iglič V, Iglič A. 1996 A simple statistical mechanical approach to the free energy of the electric double layer including the excluded volume effect. *J. Phys. II France* **6**, 477–491. (doi:10.1051/jp2:1996193)
9. Kornyshev AA. 2007 Double-layer in ionic liquids: paradigm change? *J. Phys. Chem. B* **111**, 5545–5557. (doi:10.1021/jp067857o)
10. Li B, Liu P, Xu Z, Zhou S. 2013 Ionic size effects: generalized Boltzmann distributions, counterion stratification and modified Debye length. *Nonlinearity* **26**, 2899–2922. (doi:10.1088/0951-7715/26/10/2899)
11. Levine S. 1939 On the interaction of two colloidal particles, using the complete Debye-Hückel equation. *J. Chem. Phys.* **7**, 836. (doi:10.1063/1.1750534)
12. Sharp KA, Honig B. 1990 Calculating total electrostatic energies with the nonlinear Poisson-Boltzmann equation. *J. Phys. Chem.* **94**, 7684–7692. (doi:10.1021/j100382a068)
13. Jackson JD. 1975 *Classical electrodynamics*, 2nd edn. New York, NY: Wiley.
14. Sagan H. 1969 *Introduction to the calculus of variations*. New York, NY: McGraw-Hill.
15. Debye P, Hückel E. 1923 On the theory of electrolytes. 1 Lowering of freezing point and related phenomena. *Physik. Z.* **24**, 185–206.
16. Verwey EJW, Overbeek JThG. 1948 *Theory of the stability of lyophobic colloids*. New York, NY: Elsevier.
17. Derjaguin B, Landau L. 1941 Theory of the stability of strongly charged lyophobic sols and of the adhesion of strongly charged particles in solutions of electrolytes. *Acta Physicochimica USSR* **14**, 633–662.
18. Dzyaloshinskii IE, Lifshitz EM, Pitaevskii LP. 1961 The general theory of van der Waals forces. *Adv. Phys.* **10**, 165–209. (doi:10.1080/00018736100101281)
19. McLachlan AD. 1965 Effect of the medium on dispersion forces in liquids. *Discuss. Faraday Soc.* **40**, 239–245. (doi:10.1039/df9654000239)
20. Kjellander R, Åkesson T, Jönsson B, Marčelja S. 1992 Double layer interactions in mono- and divalent electrolytes: a comparison of the anisotropic HNC theory and Monte Carlo simulations. *J. Chem. Phys.* **97**, 1424–1431. (doi:10.1063/1.463218)
21. Krumgalz BS, Pogorelsky R, Pitzer KS. 1996 Volumetric properties of single aqueous electrolytes. *J. Phys. Chem. Ref. Data* **25**, 663–689. (doi:10.1063/1.555981)

Enter a Title, ISSN, or search term to find journals or other periodicals:

[Advanced Search](#)



Search My Library's Catalog: [ISSN Search](#) | [Title Search](#)

[Search Results](#)

## Royal Society of London. Proceedings A. Mathematical, Physical and Engineering Sciences

[Title Details](#) [Table of Contents](#)

### Related Titles

[Alternative Media Edition](#) (2)

### Lists

[Marked Titles](#) (0)  
[BBA102](#) (4)

### Search History

[1364-5021](#) - (1)

[Save to List](#) [Email](#) [Download](#) [Print](#) [Corrections](#) [Expand All](#) [Collapse All](#)

### Basic Description

<b>Title</b>	Royal Society of London. Proceedings A. Mathematical, Physical and Engineering Sciences
<b>ISSN</b>	1364-5021
<b>Publisher</b>	The Royal Society Publishing
<b>Country</b>	United Kingdom
<b>Status</b>	Active
<b>Start Year</b>	1832
<b>Frequency</b>	Monthly
<b>Language of Text</b>	Text in: English
<b>Refereed</b>	Yes
<b>Abstracted / Indexed</b>	Yes
<b>Serial Type</b>	Proceedings
<b>Content Type</b>	Academic / Scholarly
<b>Format</b>	Print
<b>Website</b>	<a href="http://rspa.royalsocietypublishing.org/">http://rspa.royalsocietypublishing.org/</a>
<b>Email</b>	<a href="mailto:proca_proofs@royalsociety.org">proca_proofs@royalsociety.org</a>
<b>Description</b>	Contains papers on all aspects of the mathematical and physical sciences including chemistry and engineering at the postgraduate level and above.

### Subject Classifications

### Additional Title Details

### Title History Details

### Publisher & Ordering Details

### Price Data

### Abstracting & Indexing

### Other Availability

### Demographics

### Reviews

[Save to List](#) [Email](#) [Download](#) [Print](#) [Corrections](#) [Expand All](#) [Collapse All](#)